Supplementary Information

Philip S. Weiss,[†] Amiel S. Paz,[‡,¶,†] and Claudia. E. Avalos[*,†]

†*Department of Chemistry, New York University, New York, New York 10003, USA*

‡*NYU Shanghai, 567 West Yangsi Road, Shanghai 20012, China*

¶ *NYU-ECNU Center for Computational Chemistry at NYU Shanghai, 3663 North Zhongshang Road, Shanghai 200062, China*

E-mail: claudia.avalos@nyu.edu

Supporting Information Available

Contents

S1 Example Input Files

S1.1 TeraChem Geometry Optimizations

S1.1.1 cc-pvdz basis

```
gpus 1
basis cc-pvdz
coordinates YourStructureFile.xyz
charge 0
method uwpbeh
spinmult 2
maxit 300
convthre 6.0e-5
threall 1.0e-13
precision mixed
threspdp 1.0e-6
xtol 1.0e-5
spherical yes

run minimize
new_minimizer yes
end
```

S1.1.2 *aug*-cc-pvdz basis

```
gpus 1
basis aug-cc-pvdz
coordinates YourStructureFile.xyz
```

```
charge 0
method uwpbeh
spinmult 2
maxit 300
convthre 6.0e-5
threall 1.0e-13
precision mixed
threspdp 1.0e-6
xtol 1.0e-5
spherical yes
fock conventional

run minimize
new_minimizer yes
end
```

S1.2 Generation of Starting Orbitals with DFT in ORCA

```
%PAL NPROCS 80 END
! UKS CAM-B3LYP RIJCOSX def2-TZVP def2/J UNO UCO
! XYZFile TightSCF
%scf
MaxIter 1500
end

%maxcore 50000
```

```
%tddft nroots 40
end

* xyz 0 2
(coordinates)
*
```

S1.3 QD-NEVPT2 Calculations in ORCA

```
%PAL NPROCS 80 END
! RI-JK def2-TZVP NormalPrint MOREAD XYZFILE
%moinp "StartingOrbitals.qro"    #Or .gbw

%maxcore 45000

%basis
auxC "def2/JK"
auxJK "def2/JK"
end

* xyz 0 2
(coordinates)
*

%casscf
        trafostep ri
        nel N   #N highest electrons
```

```
        norb M   #M total orbitals
        mult 4, 2
        nroots 1, D   #D=4 in (3,3) calc's, 5 in (5,5) calc's
        PrintWF det
        ACtOrbs CanonOrbs
        PTMethod SC_NEVPT2
        PTSettings
                QDType QD_VanVleck
        end
        rel
                dosoc true
                gtensor true
        end
end

%output
Print[P_basis]2
Print[P_MOs]1
end
```

S2 XMS-CASPT2 Calculations

MS-CASPT2[25,26] calculations were conducted using the BAGEL quantum chemistry package.[27]

The CASSCF reference orbitals were converged with three-state averaging over the lowest doublet states and the XMS-CASPT2 calculations employed a 0.2 eV IPEA shift. For the quartet state, the orbitals were taken from the doublet calculation and left unoptimized.

As shown in Table S1, XMS-CASPT2 calculations on pTEMPO (structure **1a**, Figure 2) and reduced model of the ptrityl molecule (Figure S2) do very well in reproducing the 1.9997 eV (620 nm) experimentally determined singlet excitation, with errors of -0.120 eV and -0.090 eV respectively.[5]

For the case of pBDPA (**1b**) a 0.63 eV error is obtained for the main excitation. This is considerably larger than the mean absolute error in $\pi \rightarrow \pi^*$ singlet vertical excitation energies of the CASPT2 technique found by Sarkar et al.[49] (0.13 eV) or the mean unsigned deviation in $\pi \rightarrow \pi^*$ vertical excitation energies found by Schapiro et al.[50] (0.21 eV). However, the molecules of interest in this study are much larger than those tested (∼70-150 atoms as compared to less than 20) and therefore the larger errors were expected due to the greater contribution of correlation effects as N_{elec} increases. Since a reduced model of ptrityl was used, pBDPA is the largest structure among the three, and therefore greater errors were expected. Furthermore, inclusion of further orbitals has been shown to improve the energetic description of the $\pi \rightarrow \pi^*$ transition in pentacene,[52?] therefore, it was unsurprising that such a small active space did not reproduce experimental excitations accurately. In all three structures the D_1 state was found to be the trip-doublet state. This can be confirmed by looking at the configuration coefficients in the output file of, for example, **1a**, where D_1 is (denoting a configuration with $|m_{s,\pi} m_{s,R} m_{s,\pi^*}\rangle$) $\Psi_{D_1} = 0.82|\alpha\beta\alpha\rangle + 0.41|\alpha\alpha\beta\rangle + 0.41|\beta\alpha\alpha\rangle$, which agrees with the strong coupling coefficients defined in Equation 4. The trip-quartet state in the (3,3) active space can only be formed as $\Psi_{Q_0} = |\alpha\alpha\alpha\rangle$. Given that we expect **1a** and **1b** to be in the weak coupling regime ($J_{\mathrm{TR}} < 0.045$ cm^{-1}, where 0.045 cm^{-1} is the experimentally determined uniaxial ZFS splitting parameter D for pentacene[46]), and **1c** to be in an intermediate regime ($J_{\mathrm{TR}} \simeq 0.045$ cm^{-1}), it is expected that these states will be nearly degenerate since $|J_{\mathrm{TR}}| \propto E_{TQ} - E_{TD}$. Furthermore, using QD-NEVPT2 methods, Franz et al.[22] find magnitudes of J on the order of 7 cm^{-1} or less for similar systems (Figure S4). With these things in mind, the calculated splitting using XMS-CASPT2 is significantly larger than expected. One possible explanation for the error seen here in the magnetic

splitting compared to the results of Franz et al. using QD-NEVPT2 could be the use of (effectively) a one-electron in the reference Hamiltonian of CASPT2, as contrasted with the explicitly bielectronic representation in the Dyall Hamiltonian of NEVPT2.

Table S1: Calculated vertical transition energies from D_0, associated oscillator strengths (f) and J_{TR} values computed with XMS-CASPT2. Experimental absorption data gives a 2.00 eV[5] main excitation.

State	*pTEMPO (eV)*	*f*	*pBDPA (eV)*	*f*	*ptrityl* ‡ *(eV)*	*f*
Q_0	0.9506	0.0000	1.4727		0.9808	0.0000
D_1	0.9390	0.0000	0.9334	†	0.9700	0.0000
D_2	1.8799	0.1351	2.6261		1.909	0.3371
$J_{TR}(cm^{-1})$	-62.06		-6525.532		-57.73	

‡ Using reduced structure, **1c** as shown in Figure S2

† Convergence not achieved due to memory requirements.

S2.1 Example Input File for 3,3 pTEMPO CASPT2 Calculation

```
{ "bagel" : [

{
        "title" : "molecule",
        "basis" : "molden",
        "df_basis" : "cc-pvdz-jkfit",
        "angstrom" : true,
        "molden_file": "hf.molden",
       "Cartesian" : false,
        "geometry" : [

        (coodinates)

        ]
```

```
},
{
        "title" : "casscf",
        "nstate" : 3,
        "nact" : 3,
        "nclosed" : 145,
        "charge" : 0,
        "nspin" : 1,
        "natocc" : true,
        "restart_cas" : true,
        "maxiter" : 500,
        "maxiter_micro" : 300,
        "active" : [145, 147, 148]
},

{
        "title" : "print",
        "file" : "cas-mos.molden",
        "orbitals" : true
},

{
        "title" : "smith",
        "method" : "caspt2",
        "ms" : true,
        "xms" : true,
        "sssr" : true,
```

```
        "frozen" : true,
        "shift" : 0.2
},

{
        "title" : "print",
        "file" : "caspt2-mos.molden",
        "orbitals" : "true"
}
]}
```

S3 Consistency of results after geometry optimization with an alternate functional.

In order to study the effects on J_{TR} of using a different functional for the cc-pvdz and *aug*-cc-pvdz steps of the geometry optimization, structures **1a**, **1b**, and **1c** were reoptimized from their UB3LYP/6-31G(d) structures (once again on TeraChem) using the UωB97X-D_3 functional.[47,48] We find that J_{TR} values remained consistent to at least 10^{-3} $cm*-1$ ($\sim$30 MHz) when UωB97X-D_3 was used for optimization. J_{TR} of structure **1a** changed in magnitude to -0.0035731 cm^{-1}, a difference of about -0.002 cm^{-1}, structure **1b** to -0.0008998 cm^{-1} for a difference of about 0.0000761 cm^{-1}, and structure **1c** to -0.0117846 cm^{-1} for a difference of about 0.0080520 cm^{-1}. One may expect nontrivial energetic differences between marginally different geometries due to the sensitivity of perturbation methods in near-degeneracies and the high number of electrons, N_{elec}; it was therefore pleasantly surprising to see such small variance in the (3,3) QD-NEVPT2 J_{TR} values predicted for each structure, and implies that the method is robust with respect to the description of close magnetic splittings for these

structures. For reference, k_BT here for T = 85 K (the temperature at which EPR measurements were taken in Ref.[5]) is about 0.007324 eV, or about 59.08 cm^{-1}, and therefore the largest difference in J_{TR} between optimization functionals was seen in the trityl-tethered structure **1c** at 0.008 cm^{-1}, only 0.013% of k_BT.

S4 Method of Calculating Spin Centroids

Structures were divided into two regions *via* inspection of the structure in GaussView 6, with the partiton being between the pentacene/bridge moieties and the radical. Using QD-NEVPT2 calculated Löwdin spin densities, and approximating atom coordinates as points of spin density, the following equation was used to calculate centroids of triplet or radical spin density in their respective regions:

$$\begin{aligned} \bar{x}^{T/R} = (\rho_{Tot}^{T/R})^{-1}(\sum_i x_i^{T/R} * \rho_{\vec{\sigma},i}^{T/R}) \\ \bar{y}^{T/R} = \dots \\ \bar{z}^{T/R} = \dots \end{aligned} \tag{S1}$$

where $\bar{x}^{T/R}$ represents the spin density centroid in the x coordinate of the triplet / radical moieties respectively, x_i is the x-coordinate of atom i, $\rho_{\vec{\sigma},i}$ is the Löwdin spin density on atom center i, and $\rho_{Tot}^{T/R}$ is the total spin density (summed over atom centers) on the fragment. $\bar{y}^{T/R}$ and $\bar{z}^{T/R}$ are found similarly.

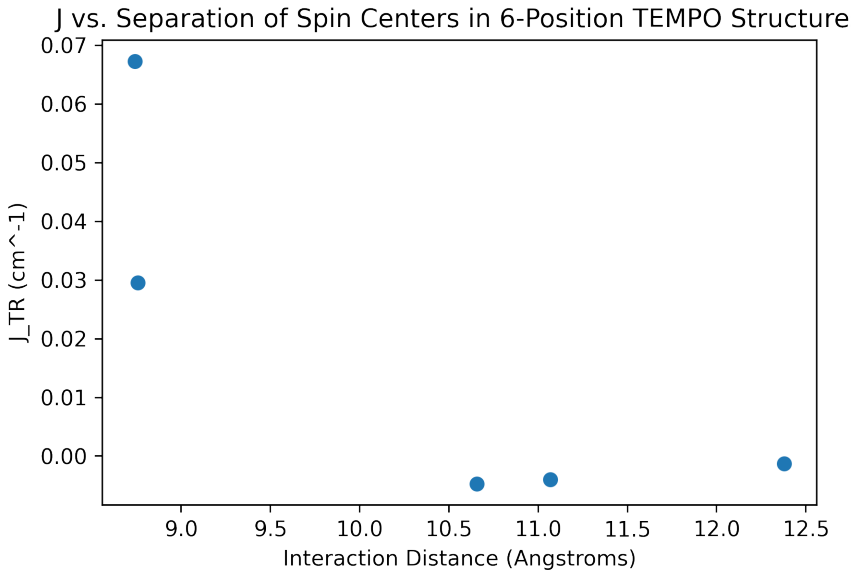

Figure S1: Graph for pTEMPO structures showing J_{TR} versus spin centroid distance for pTEMPO structures **1,2,3,6,7a**

S5 Supplementary Figures

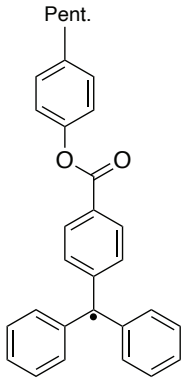

Figure S2: Structure of **1c** cut-down structure used for XMS-CASPT2 calculation on BAGEL.

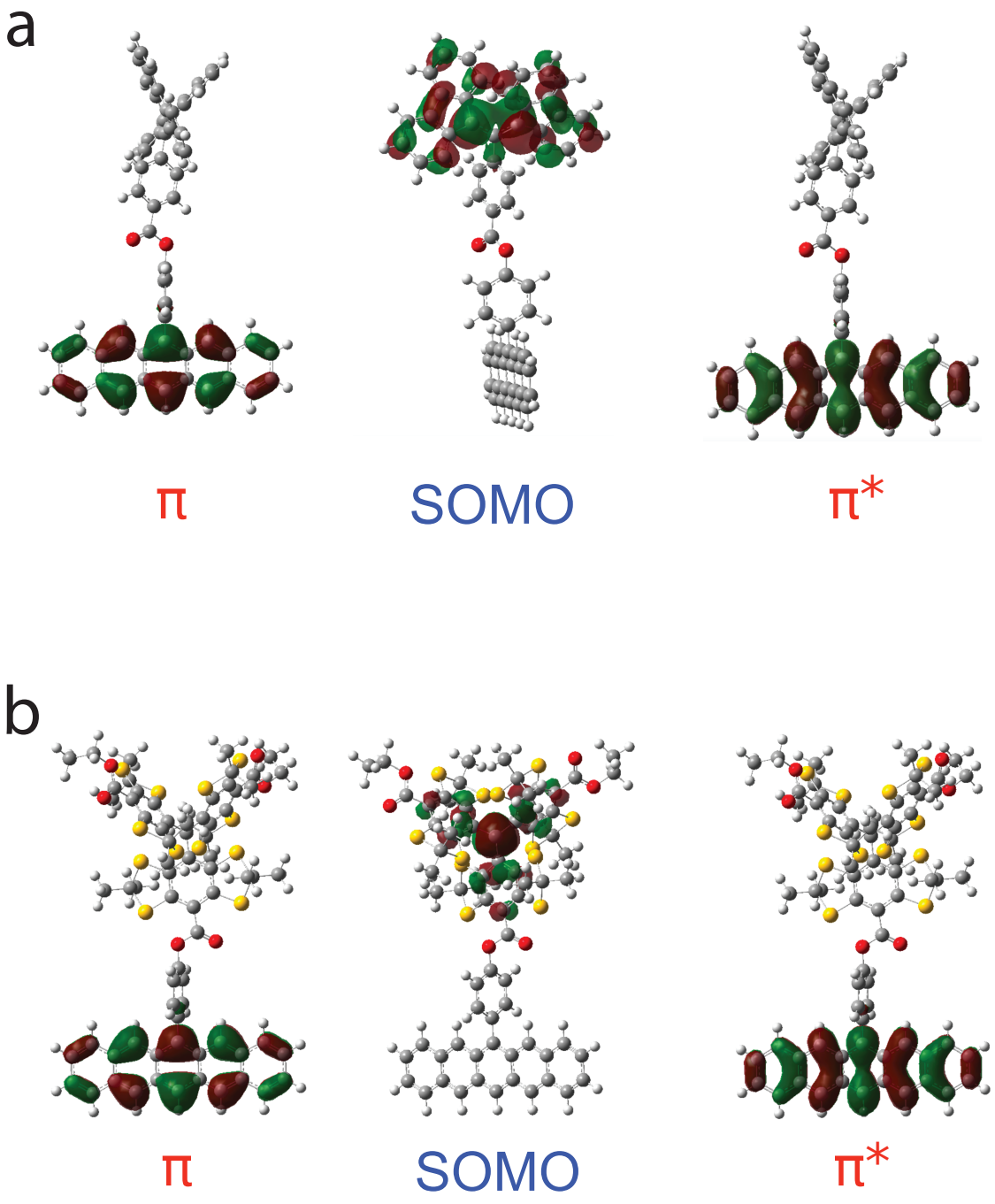

Figure S3: CASSCF orbitals of **a, 1b** and **b, 1c** resulting from (3,3) QDNEVPT2 calculations.

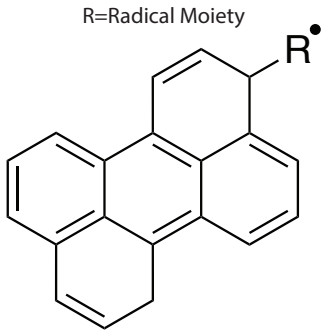

Figure S4: Structure of perylene chromophore used as tether for radicals in Franz et al.[22]

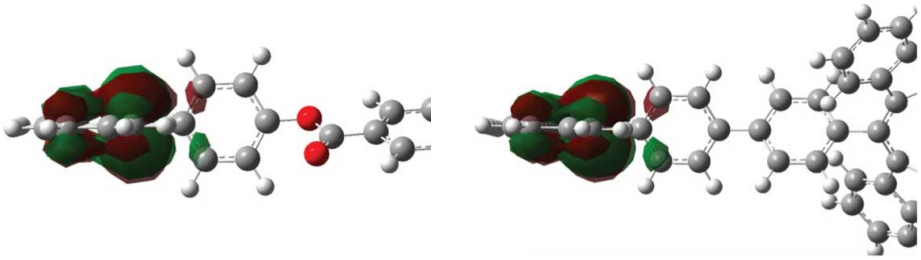

Figure S5: Pentacene HOMO π orbital in pBDPA structures **1b** (left) and **2b** (right).

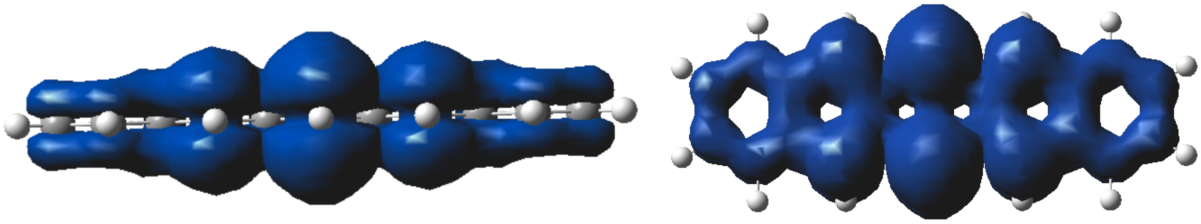

Figure S6: Spin density plots of lone pentacene from a QD-NEVPT2 calculation converging to the lowest triplet state.

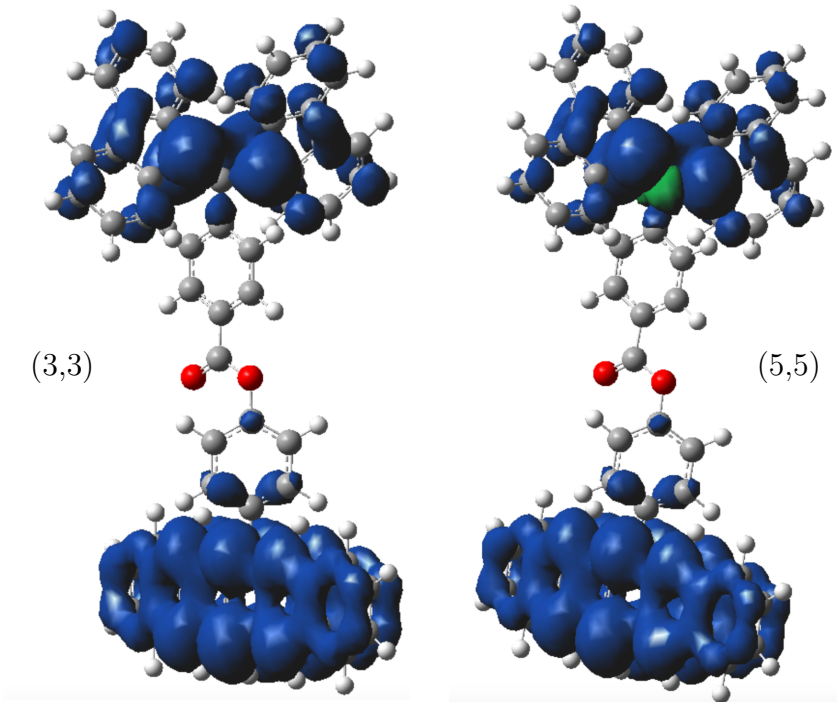

Figure S7: Spin density plots of BDPA structure **1b*** resulting from a (3,3) QDNEVPT2 (left) versus a (5,5) QDNEVPT2 (right) calculation.

S6 Supplementary Data

Table S2: Calculated state absolute energies and J_{TR} values computed with XMS-CASPT2

	pTEMPO [1a] (eV)	*pBDPA [1b] (eV)*	*ptrityl* (eV)*
D_0	-1743.66292612080	-2527.700116124000	-1992.1704516582
D_1	-1743.62698929900	-2527.665815966600	-1992.1347982935
Q_0	-1743.610784972500	-2527.645994758300	-1992.1344037750
D_2	-1743.59241355540	-2527.603607801700	-1992.1002728221
J_{TR} *(cm^{-1})*	-2371.015	-6525.532	-57.536

*Cut-down structure of ptrityl given in Figure S2

Table S3: Calculated absolute energies and J_{TR} values computed with (3,3) QD-NEVPT2.

	pTEMPO [1a] (eV)	*pBDPA [1b] (eV)*	*ptrityl [1c] (eV)*
D_0	-1745.275832367070	-2530.017233915170	-7998.934201388510
D_1	-1745.228098572030	-2529.970996154010	-7998.886663746730
Q_0	-1745.228098563490	-2529.970996147340	-7998.886663721220
D_2	-1745.220491422600	-2529.965305739120	-7998.879179691240
D_3	-1745.197612489720	-2529.949511547330	-7998.856286971140
J_{TR} *(cm^{-1})*	-0.001366636	-0.000975921	-0.003732548

Table S4: Calculated absolute energies and J_{TR} values computed with (3,3) QD-NEVPT2 without carboxylate bridging component.

	pTEMPO [2a] (eV)	*pBDPA [2b] (eV)*	*ptrityl [2c] (eV)*
D_0	-1556.996027448170	-2341.73989140614	-7810.662360182030
D_1	-1556.948223787700	-2341.69729276581	-7810.614795670480
Q_0	-1556.948223755420	-2341.69729496954	-7810.614791396890
D_2	-1556.940735440200	-2341.69203999963	-7810.607545608140
D_3	-1556.917830407660	-2341.67751284116	-7810.584781801260
J_{TR} *(cm^{-1})*	-0.004717352	0.322178774	-0.626009

Table S5: Calculated absolute energies and J_{TR} values computed with (3,3) QD-NEVPT2 with a phenyl-carbonyl bridging component.

	pTEMPO [3a] (eV)	*pBDPA [3b] (eV)*	*ptrityl [3c] (eV)*
D_0	-1670.145990376590	-2454.885609499	-7923.808625288320
D_1	-1670.098173348270	-2454.839119799	-7923.761049557040
Q_0	-1670.098173320970	-2454.839119758	-7923.761049286170
D_2	-1670.090807384460	-2454.833711804	-7923.753934328680
D_3	-1670.067741034790	-2454.820743947	-7923.730991411210
J_{TR} (cm^{-1})	-0.003994510176	-0.006102984487	-0.03963356815

Table S6: Calculated absolute energies and J_{TR} values computed with (3,3) QD-NEVPT2 with bridge attachment at 2-position of pentacene.

	pTEMPO [4a] (eV)	*pBDPA [4b] (eV)*	*ptrityl [4c] (eV)*
D_0	-1745.273022080620	-2530.015295999750	-7998.930991686620
D_1	-1745.225583845780	-2529.969003693660	-7998.883821577870
Q_0	-1745.225583829420	-2529.969002777370	-7998.883819915270
D_2	-1745.213005792730	-2529.957933049560	-7998.871227467170
D_3	-1745.191191253890	-2529.934749840300	-7998.849586217660
J_{TR} (cm^{-1})	-0.0023894	-0.134071433	-0.244335098

Table S7: Calculated absolute energies and J_{TR} values computed with (3,3) QD-NEVPT2 for bridge attachment at 2-position of pentacene with the carboxylate bridge linker removed.

	pTEMPO [5a] (eV)	*pBDPA [5b] (eV)*	*ptrityl [5c] (eV)*
D_0	-1556.993488457270	-2341.737743142	-7810.658962461200
D_1	-1556.946122628880	-2341.691446219	-7810.611868289700
Q_0	-1556.946122611990	-2341.691446018	-7810.611861389520
D_2	-1556.933539965720	-2341.680403369	-7810.599261254260
D_3	-1556.911785372030	-2341.657305763	-7810.577644576140
J_{TR} (cm^{-1})	-0.00247134	0.02946008	-1.00963355

Table S8: Calculated absolute energies and J_{TR} values computed with (3,3) QD-NEVPT2 for pTEMPO, pBDPA, and ptrityl with an Alkyne bridge.

	pTEMPO [6a] (eV)	*pBDPA [6b] (eV)*	*ptrityl [6c] (eV)*
D_0	-1402.442193432400	-2187.187443205	-7656.116720208980
D_1	-1402.396464943380	-2187.144034757	-7656.079768361770
Q_0	-1402.396465403480	-2187.144106480	-7656.076284940870
D_2	-1402.387909539760	-2187.138559642	-7656.072186329800
D_3	-1402.364123141980	-2187.137422019	-7656.049009003480
J_{TR} (cm^{-1})	0.06732179891	10.49450591	-509.6936940

Table S9: Calculated absolute energies and J_{TR} values computed with (3,3) QD-NEVPT2 for pTEMPO, pBDPA, and ptrityl with an alkyne – carbonyl bridging component.

	pTEMPO [7a] (eV)	*pBDPA [7b] (eV)*	*ptrityl [7c] (eV)*
D_0	-1402.442193432400	-2187.187443205	-7656.116720208980
D_1	-1402.396464943380	-2187.144034757	-7656.079768361770
Q_0	-1402.396465403480	-2187.144106480	-7656.076284940870
D_2	-1402.387909539760	-2187.138559642	-7656.072186329800
D_3	-1402.364123141980	-2187.137422019	-7656.049009003480
J_{TR} (cm^{-1})	0.06732179891	10.49450591	-509.6936940

Table S10: Calculated absolute energies and J_{TR} values computed with (3,3) QD-NEVPT2 for attachment at the 2-position with an alkyne bridging component.

	pTEMPO [8a] (eV)	*pBDPA [8b] (eV)*	*ptrityl [8c] (eV)*
D_0	-1402.436632536710	-2187.182383258	-7656.104023340010
D_1	-1402.389334921260	-2187.136217666	-7656.057621306730
Q_0	-1402.389334967560	-2187.136229753	-7656.057153323100
D_2	-1402.376742081450	-2187.125251969	-7656.045015833400
D_3	-1402.355237181000	-2187.114998408	-7656.023721322240
J_{TR} (cm^{-1})	0.006774624847	1.768508248	-68.4753040

Table S11: Calculated absolute energies and J_{TR} values computed with (3,3) QD-NEVPT2 for pBDPA and ptrityl with an *m*-phenyl-carboxylate bridging component.

	pTEMPO [9a] (eV)	*pBDPA [9b] (eV)*	*ptrityl [9c] (eV)*
D_0	-2530.020388523190	-7998.949643201760	
D_1	-2529.972453571960	-7998.944595582160	
Q_0	-2529.972453536520	-7998.897068816780	
D_2	-2529.965141137420	-7998.897068575380	
D_3	-2529.955155356130	-7998.890044058030	
D_4	-2529.942154760050	-7998.866811439150	
J_{TR} (cm^{-1})	-0.005185617176	0.03532160244	

Table S12: Calculated absolute energies and J_{TR} values computed with (3,3) QD-NEVPT2 for pBDPA and ptrityl with an *m*-phenyl bridging component.

	pTEMPO [10a] (eV)	*pBDPA [10b] (eV)*	*ptrityl [10c] (eV)*
D_0	-2341.742588102280	-7810.673278644640	
D_1	-2341.694547074310	-7810.671833377810	
Q_0	-2341.694546816990	-7810.624644358950	
D_2	-2341.687528008210	-7810.624643883270	
D_3	-2341.680201266020	-7810.617802862870	
D_4	-2341.664414850270	-7810.594879207220	
J_{TR} (cm^{-1})	-0.03765098481	0.06960134389	

Table S13: Calculated absolute energies and J_{TR} values computed with (3,3) QD-NEVPT2 for pBDPA and ptrityl with an alkyne-*m*-phenyl bridging component.

	pTEMPO [11a] (eV)	*pBDPA [11b] (eV)*	*ptrityl [11c] (eV)*
D_0	-2417.740822141940	-7886.675553945590	
D_1	-2417.695695618540	-7886.673964555620	
Q_0	-2417.695691533460	-7886.629255163770	
D_2	-2417.688242621640	-7886.629245253660	
D_3	-2417.676389711350	-7886.621939917670	
D_4	-2417.663495640940	-7886.597584200080	
J_{TR} *(cm^{-1})*	-0.5977283807	1.450045985	

Table S14: Weighting coefficients for configurations $|T_+,\beta\rangle$, $|T_0^{\uparrow(\downarrow^*)},\alpha\rangle$, and $|T_0^{\downarrow(\uparrow^*)},\alpha\rangle$ associated with the trip-doublet state calculated from (3,3) QD-NEVPT2 calculations

	$C_{\lvert T_+,\beta\rangle}$	$C_{\lvert T_0^{\uparrow(\downarrow^*)},\alpha\rangle}$	$C_{\lvert T_0^{\downarrow(\uparrow^*)},\alpha\rangle}$	$\frac{(C_{\lvert T_+,\beta\rangle})^2}{(C_{\lvert T_0^{\uparrow(\downarrow^*)},\alpha\rangle})^2+(C_{\lvert T_0^{\downarrow(\uparrow^*)},\alpha\rangle})^2}$
1a	-0.816496567	0.408246284	0.408250283	2.0000000
1a*	0.816495628	-0.408244802	-0.408250826	2.0000000
1b	-0.816496569	0.408249384	0.408247185	2.0000000
1b*	-0.816495932	0.408289180	0.408206752	2.0000000
1c	0.816472506	-0.408229333	-0.408243173	2.0000000
1c*	-0.811051731	0.408310640	0.402741092	1.9999057
2a	-0.816496196	0.408251269	0.408244927	2.0000000
2b	-0.816496569	0.408244640	0.408251929	2.0000000
2c	0.815847788	-0.408213949	-0.407633839	1.9999990
3a	0.816495761	-0.408239722	-0.408256039	2.0000000
3b	0.816495676	-0.408241422	-0.408254253	2.0000000
3c	0.816368065	-0.408237682	-0.408130383	2.0000000
6a	-0.816496570	0.408235592	0.408260978	2.0000000
6b	-0.816494934	0.407497890	0.408997043	1.9999933
6c	-0.411405458	0.375810147	0.035595311	1.1877481
7a	0.816453188	-0.408237614	-0.408215575	2.0000000
7b	-0.816377225	0.408113734	0.408263490	1.9999999
7c	0.794324834	-0.412800373	-0.381524461	1.9969041

Table S15: Calculated absolute energies and J_{TR} values computed with (5,5) QD-NEVPT2.

	pBDPA [1b] (eV)	*ptrityl [1c] (eV)*
D_0	-2529.991245027680	-7998.953422042780
D_1	-2529.945032694280	-7998.943772269090
Q_0	-2529.943938506380	-7998.896201032880
D_2	-2529.943939358520	-7998.896200088520
D_3	-2529.906856980840	-7998.895563248890
D_4	-2529.859555995850	-7998.857861563480
J_{TR} *(cm^{-1})*	-0.1246849692	-0.1381785261

Table S16: Calculated absolute energies and J_{TR} values computed with (5,5) QD-NEVPT2 for angle-adjusted structures.

	pBDPA [1b] (eV)*	*ptrityl [1c*] (eV)*
D_0	-2529.982181390570	-7998.924533963710
D_1	-2529.935891772260	-7998.878608264290
Q_0	-2529.935481071100	-7998.877765607060
D_2	-2529.935482728980	-7998.877774976470
D_3	-2529.897825255890	-7998.859902050770
D_4	-2529.851134364360	-7998.8131377070300
J_{TR} (cm^{-1})	-0.2425807415	-1.370930956

Table S17: Calculated absolute energies and J_{TR} values computed with (5,5) QD-NEVPT2 without carboxylate bridging component.

	pBDPA [2b] (eV)	*ptrityl [2c] (eV)*
D_0	-2341.7134955127	-7810.677276258120
D_1	-2341.6701091418	-7810.672400708320
Q_0	-2341.6717205859	-7810.624800840580
D_2	-2341.6701055697	-7810.624793681000
D_3	-2341.6294596992	-7810.624540141350
D_4	-2341.5861314690	-7810.588499661850
J_{TR} (cm^{-1})	0.5226677465	-1.0475889

Table S18: Calculated absolute energies and J_{TR} values computed with (5,5) QD-NEVPT2 with bridge attachment at 2-position of pentacene.

	pBDPA [4b] (eV)	*ptrityl [4c] (eV)*
D_0	-2529.9895020017	-7998.952833368080
D_1	-2529.9418958991	-7998.941233758690
Q_0	-2529.9418953145	-7998.893204975300
D_2	-2529.9359389133	-7998.893200649090
D_3	-2529.9051036770	-7998.885824204930
D_4	-2529.8574693510	-7998.855501628450
J_{TR} (cm^{-1})	-0.08554884339	-0.6330105

Table S19: Calculated absolute energies and J_{TR} values computed with (5,5) QD-NEVPT2 for bridge attachment at 2-position of pentacene with the carboxylate bridge linker removed (no convergence on 5c).

	pBDPA [5b] (eV)	*ptrityl [5c] (eV)*
D_0	-2341.7117989146	
D_1	-2341.6639888318	
Q_0	-2341.6639902128	
D_2	-2341.6575444727	
D_3	-2341.6280752807	
D_4	-2341.5803316101	
J_{TR} (cm^{-1})	0.2020662692	

Table S20: Calculated absolute energies and J_{TR} values computed with (5,5) QD-NEVPT2 for pTEMPO, pBDPA, and ptrityl with an Alkyne bridge.

	pBDPA [6b] (eV)	*ptrityl [6c] (eV)*
D_0	-2187.161262604910	-7656.110638315320
D_1	-2187.116609271740	-7656.074644204960
Q_0	-2187.116792451330	-7656.071214645510
D_2	-2187.114396724850	-7656.070415270350
D_3	-2187.077586660760	-7656.043719491380
D_4	-2187.034636872760	-7656.006364154390
J_{TR} (cm^{-1})	26.80281388	-501.8126937

Table S21: Calculated absolute energies and J_{TR} values computed with (5,5) QD-NEVPT2 for pTEMPO, pBDPA, and ptrityl with an alkyne-carbonyl bridging component.

	pBDPA [7b] (eV)	*ptrityl [7c] (eV)*
D_0	-2300.306487303570	-7769.261595047090
D_1	-2300.262003629580	-7769.243270620870
Q_0	-2300.262012507150	-7769.218545435630
D_2	-2300.256418523350	-7769.218545435630
D_3	-2300.221381397130	-7769.218229125480
D_4	-2300.177488888300	-7769.21026614676
J_{TR} (cm^{-1})	-1.298964898	46.2824601

Table S22: Calculated absolute energies and J_{TR} values computed with (5,5) QD-NEVPT2 for attachment at the 2-position with an alkyne bridging component (no convergence on 8c).

	pBDPA [8b] (eV)	*ptrityl [8c] (eV)*
D_0	-2187.1561145189	
D_1	-2187.1083399058	
Q_0	-2187.1083673005	
D_2	-2187.1020354856	
D_3	-2187.0722872883	
D_4	-2187.0247569127	
J_{TR} *(cm^{-1})*	4.008396243	

Table S23: Calculated absolute energies and J_{TR} values computed with (5,5) QD-NEVPT2 for m-phenyl-carboxylate linker.

	pBDPA [9b] (eV)	*ptrityl [9c] (eV)*
D_0	-2529.992140415580	-7998.932319327040
D_1	-2529.945724206050	-7998.887014281980
Q_0	-2529.944702872610	-7998.885282005080
D_2	-2529.944702101810	-7998.885278968660
D_3	-2529.907876143580	-7998.867300177440
D_4	-2529.860462432040	-7998.820235503050
J_{TR} *(cm^{-1})*	-0.1127833476	-0.4442885674

Table S24: Calculated absolute energies and J_{TR} values computed with (5,5) QD-NEVPT2 for m-phenyl linker.

	pBDPA [10b] (eV)	*ptrityl [10c] (eV)*
D_0	-2341.714333542040	-7810.680307635600
D_1	-2341.667542985280	-7810.675024400920
Q_0	-2341.666809529710	-7810.627458305660
D_2	-2341.666807311970	-7810.627480253130
D_3	-2341.630321433490	-7810.627400470250
D_4	-2341.582796948360	-7810.591217322130
J_{TR} *(cm^{-1})*	-0.32449944	-3.2113509

Table S25: Calculated absolute energies and J_{TR} values computed with (5,5) QD-NEVPT2 for Alkyne-m-phenyl linker.

	pBDPA [11b] (eV)	*ptrityl [11c] (eV)*
D_0	-2417.712135421770	-7886.681126216590
D_1	-2417.667815261340	-7886.676288034940
Q_0	-2417.667812765400	-7886.631944748460
D_2	-2417.665776431090	-7886.631936900370
D_3	-2417.627859619790	-7886.629433139180
D_4	-2417.583655120750	-7886.592090792590
J_{TR} (cm^{-1})	-0.3652056099	1.148331482

Table S26: Calculated QD-NEVPT2 oscillator strengths associated with each Doublet excitation from D_0 for structures 1a through 11c with (3,3) active space.

	D_1	D_2	D_3
1a	0.000000000	0.221541740	0.000978972
1b	0.000000000	0.127515641	0.000000027
1c	0.000000000	0.222994234	0.000827292
2a	0.000000000	0.352831319	0.000000638
2b	0.000000000	0.349100031	0.000032095
2c	0.000000000	0.220982248	0.000728215
3a	0.000000000	0.221186363	0.001570659
3b	0.000000000	0.128446583	0.000000107
3c	0.000000000	0.222824819	0.001142254
4a	0.000000000	0.215136728	0.000053670
4b	0.000000003	0.136030609	0.000000362
4c	0.000000004	0.213395741	0.000036400
5a	0.000000000	0.214755968	0.000066465
5b	0.000000080	0.135778548	0.000016450
5c	0.000000015	0.213080422	0.000012467
6a	0.000000000	0.271628908	0.002675916
6b	**0.000000289**	**0.000477993**	**0.185695656**
6c	0.000036981	0.295109272	0.005304581
7a	0.000000000	0.284572327	0.012341354
7b	0.000000046	0.187354218	0.000052721
7c	0.000031614	0.281237334	0.012579296
8a	0.000000000	0.211389189	0.000044095
8b	0.000000237	0.133400703	0.000160068
8c	0.000012782	0.205940551	0.000178003
9b	0.000000000	0.352044845	0.000000305
9c	0.000000000	0.362090510	0.001027612
10b	0.000000001	0.351295807	0.000101949
10c	0.000000000	0.362090510	0.001027612
11b	0.000000000	0.485056795	0.000005229
11c	0.000000000	0.482592560	0.002013120

Table S27: Calculated QD-NEVPT2 oscillation frequencies associated with each Doublet excitation from D_0 for (5,5) active space trityl and BDPA structures. Structures **5c** and **8c** did not reach CASSCF convergence.

	D_1	D_2	D_3	D_4
1b	0.1118893	0.0000000	0.0019128	0.0000000
1b*	0.1214947	0.0000000	0.0018685	0.0000000
1c	0.0038551	0.0000000	0.1184209	0.1839790
1c*	0.1211797	0.0000070	0.0138689	0.0000000
2b	0.0996821	0.0000000	0.0030155	0.0000000
2c	0.0020824	0.0000000	0.0001363	0.0002910
4b	0.0000000	0.1250462	0.0019632	0.0000000
4c	0.0042329	0.0000000	0.0000530	0.0000798
5b	0.0000000	0.1264284	0.0030864	0.0000000
5c	———-	———-	———-	———-
6b	0.0000002	0.1677881	0.0025546	0.0000066
6c	0.0006256	0.1662815	0.0130010	0.0001093
7b	0.0000001	0.1802895	0.0021065	0.0000000
7c	0.0063834	0.0304868	0.0032960	0.1632323
8b	0.0000001	0.1247690	0.0026587	0.0000002
8c	———-	———-	———-	———-
9b	0.1124615	0.0000000	0.0019410	0.0000000
9c	0.1135004	0.0000000	0.0136985	0.0000000
10b	0.1136219	0.0000002	0.0029984	0.0000000
10c	0.0022005	0.0000001	0.0000101	0.0000562
11b	0.0000000	0.1626622	0.0029415	0.0000000
11c	0.0020673	0.0000000	0.0001059	0.0000387